Cell Host & Microbe
Article

Fusobacterium nucleatum Promotes Colorectal Carcinogenesis by Modulating E-Cadherin/β-Catenin Signaling via its FadA Adhesin

Mara Roxana Rubinstein,[1,7] Xiaowei Wang,[1,7] Wendy Liu,[2] Yujun Hao,[3,5] Guifang Cai,[6] and Yiping W. Han[1,2,4,*]
[1]Department of Periodontics
[2]Department of Pathology
[3]Department of Genetics and Genome Sciences
[4]Department of Reproductive Biology
[5]Case Comprehensive Cancer Center
[6]School of Dental Medicine
Case Western Reserve University, Cleveland, OH 44106, USA
[7]These authors contributed equally to this work
*Correspondence: yiping.han@case.edu
http://dx.doi.org/10.1016/j.chom.2013.07.012

SUMMARY

Fusobacterium nucleatum **(*Fn*) has been associated with colorectal cancer (CRC), but causality and underlying mechanisms remain to be established. We demonstrate that *Fn* adheres to, invades, and induces oncogenic and inflammatory responses to stimulate growth of CRC cells through its unique FadA adhesin. FadA binds to E-cadherin, activates β-catenin signaling, and differentially regulates the inflammatory and oncogenic responses. The FadA-binding site on E-cadherin is mapped to an 11-amino-acid region. A synthetic peptide derived from this region of E-cadherin abolishes FadA-induced CRC cell growth and oncogenic and inflammatory responses. The *fadA* gene levels in the colon tissue from patients with adenomas and adenocarcinomas are >10–100 times higher compared to normal individuals. The increased FadA expression in CRC correlates with increased expression of oncogenic and inflammatory genes. This study unveils a mechanism by which *Fn* can drive CRC and identifies FadA as a potential diagnostic and therapeutic target for CRC.**

INTRODUCTION

The human intestinal microbiome contains >1,000 different species, totaling 10^{14} microorganisms, and plays an extremely important role in the maintenance of the normal physiology of the gut, including energetic metabolism, proliferation and survival of epithelial cells, and protection against pathogens (Tremaroli and Bäckhed, 2012). The microbiota exerts both beneficial and detrimental effects on host contributing to health or disease (Sekirov et al., 2010). Recently, two research teams simultaneously reported overabundance of a specific microorganism, *Fusobacterium nucleatum* (*Fn*), in colorectal carcinoma tissues (Castellarin et al., 2012; Kostic et al., 2012). However, it was unknown if *Fn* was a cause or a consequence of CRC.

Fn is an opportunistic commensal anaerobe in the oral cavity, implicated in various forms of periodontal diseases. Outside the oral cavity, it is one of the most prevalent species in extraoral infections (Han, 2011). It is highly prevalent in intrauterine infection associated with pregnancy complications such as preterm birth, stillbirth, and neonatal sepsis (Han et al., 2009; 2010; Wang et al., 2013). *Fn* adheres to and invades endothelial and epithelial cells, a mechanism likely utilized for its systemic dissemination (Han et al., 2000; 2004). The attachment and invasion take place via adhesin FadA, a virulence factor identified from *Fn* (Han et al., 2005; Xu et al., 2007). Immunofluorescent staining of nonpermeabilized *Fn* using anti-FadA monoclonal antibodies showed that FadA is expressed on the bacterial surface (Ikegami et al., 2009).

FadA is highly conserved among *Fn* (Han et al., 2005). It exists in two forms: the nonsecreted intact pre-FadA consisting of 129 amino acid (aa) residues and the secreted mature FadA (mFadA) consisting of 111 aa without the 18 aa signal sequence (Han et al., 2005). The mFadA monomer is predominantly α-helical and forms a hairpin-like structure (Nithianantham et al., 2009). The monomers are linked together in a head-to-tail pattern to form uniformly long and thin filaments, with no binding activity (Témoin et al., 2012). When mFadA is mixed with pre-FadA, they form active complex FadAc, consisting of heterogeneous filaments, presumably due to varying degrees of filament bundling (Xu et al., 2007; Témoin et al., 2012). We have recently demonstrated that the vascular endothelial (VE) cadherin (CDH5), a member of the cadherin superfamily, is a receptor for FadA that is required for *Fn* to attach and invade endothelial cells (Fardini et al., 2011). The receptor for FadA on epithelial cells was not identified.

In the present study, we demonstrate that FadA binds to E-cadherin on CRC and non-CRC cells, mediating *Fn* attachment of and invasion into the epithelial cells. FadA modulates E-cadherin and activates β-catenin signaling, leading to increased expression of transcription factors, oncogenes, Wnt genes, and inflammatory genes, as well as growth stimulation of CRC cells. Further, we show that while FadA binding to CRC

cells is sufficient to turn on the Wnt and oncogenes, its internalization mediated by clathrin is needed to activate the inflammatory genes. This study reveals a mechanism by which *Fn* contributes to CRC and identifies FadA as a potential diagnostic and therapeutic target for CRC.

RESULTS

Fn Stimulates Human CRC Cell Proliferation

Wild-type *Fn* 12230 significantly stimulated proliferation of human colon cancer cells HCT116, DLD1, SW480, and HT29, but only weakly stimulated RKO. It did not stimulate the noncancerous human embryonic kidney (HEK) 293 cells. Compared to the untreated cells or those incubated with *E. coli* DH5α, the growth stimulation increased by approximately 100% for HCT116, DLD1, SW480, and HT29, but only 18% for RKO, after 72 hr (Figure 1A). The *fadA*-deletion mutant US1 weakly stimulated the growth of all cancer cell lines. The *fadA*-complementing clone USF81 restored proliferation of HCT116, DLD1, SW480, and HT29 to the wild-type level. Furthermore, HCT116 growth was enhanced by purified FadAc in a dose-dependent manner, with the maximum stimulation observed at 1 mg/ml, while mFadA exhibited no stimulatory effect (Figure 1B). Neither FadAc nor mFadA stimulated growth of RKO. These results indicate that stimulation of CRC cells by *Fn* is FadA dependent.

FadA Binds to E-Cadherin on CRC Cells

To investigate the mechanism by which FadA stimulates CRC cell growth, we set out to identify CRC cell receptors for FadA. It was previously shown that FadA binds to VE-cadherin on endothelial cells (Fardini et al., 2011). Cadherins are a large family of calcium-dependent cell adhesion glycoproteins, each composed of five extracellular repeat domains (EC1–EC5), a transmembrane domain, and a highly conserved cytoplasmic tail that binds other cytoplasmic components including β-catenin (Gumbiner, 2005) (Figure 2A). Given the 33.5% similarity between VE- and endothelial (E)-cadherins, we speculated as to whether FadA also bound to E-cadherin. E-cadherin is present at different levels on epithelial cells, including the noncancerous HEK 293 and the CRC cells, except RKO (Figure 2B). FadA binding to E-cadherin was directly tested by coimmunoprecipitation. FadAc coprecipitated with E-cadherin, while mFadA did not (Figure 2C). Using the glutathione S-transferase (GST) pull-down assay, we determined that FadAc bound specifically to EC5 of E-cadherin, but not to EC1–EC4, the transmembrane, or the cytoplasmic domains (Figure 2D). Deletions of various regions in EC5 showed that region 3 was responsible for FadA binding (Figure S2 available online; see also below).

FadA Promotes *Fn* Attachment and Invasion of E-Cadherin-Expressing Cells

Attachment and invasion are hallmarks of *Fn*. Thus, we tested the role of FadA binding to E-cadherin in these processes. *Fn* attachment and invasion of noncancerous HEK 293 cells was inhibited by mouse monoclonal antibody HECD-1 raised against the extracellular domain of E-cadherin (Figure S3A). Deletion of *fadA* (US1) severely impaired the ability of *Fn* to bind and invade HEK 293, whereas the *fadA*-complemented clone USF81 restored the activities. Downregulation of E-cadherin expression by small interfering RNA (siRNA) in HEK 293 significantly inhibited attachment and invasion by wild-type *Fn* and USF81 (Figure S3B). These results indicate that *Fn* attachment and invasion of HEK 293 requires FadA and E-cadherin.

Similar observations were made with CRC HCT116 cells expressing E-cadherin. US1 (*fadA*$^{-}$) was defective in the attachment and invasion of HCT116, compared to wild-type *Fn* or USF81 (*fadA*$^{+}$) (Figure 3A). Inhibition of E-cadherin expression by siRNA reduced attachment and invasion (Figure 3A). In contrast, no difference was observed among *Fn* 12230, US1, and USF81 in their weak binding and invasion of the non-E-cadherin-expressing RKO cells (Figure 3B). Transfection of RKO with the full-length E-cadherin led to increased binding and invasion by *Fn* 12230 and USF81 to levels comparable to those observed in HCT116 (Figure 3B). These results indicate that FadA mediates *Fn* attachment and invasion of CRC cells via E-cadherin.

E-cadherin can be internalized via clathrin (Bryant and Stow, 2004). Pitstop2, a clathrin inhibitor (von Kleist et al., 2011), prevented *Fn* invasion of HCT116 without affecting attachment (Figure 3C). *Fn* stimulated expression of the inflammatory genes, including NF-κB and cytokines interleukin-6 (IL-6), IL-8, and IL-18 from HCT116 (Figure 3D). Such stimulation was abolished in the presence of the clathrin inhibitor, indicating that invasion was required for the stimulation of inflammation (Figure 3D).

Identification of Inhibitory Peptides to Prevent *Fn* Attachment and Invasion

Since FadA bound to the EC5 domain of E-cadherin, we tested the role of EC5 in *Fn* attachment and invasion. *Fn* attachment and invasion of HCT116 was inhibited by purified GST-EC5 fusion protein in a dose-dependent manner, with maximum inhibition observed at 0.1 mM (Figures 4A and 4B). Synthetic peptides derived from different regions of EC5 were then tested for their ability to inhibit *Fn* attachment and invasion (Figures 4A and 4C). Peptide 3, corresponding to region 3, exhibited inhibitory effects similar to those of EC5 (Figure 4C). To determine the minimal sequences required for inhibition, sequential deletions of peptide 3 were generated. The results showed that the 11 aa peptide (ASANWTIQYND) was the minimum required and was designated as the inhibitory peptide (IP) (Figure 4D).

FadA Promotes CRC Cell Proliferation via E-Cadherin

Stimulation of HCT116 growth by *Fn* was inhibited by the CDH1-specific siRNA, EC5, and the inhibitory peptide (Figure 1C). In the non-E-cadherin-expressing RKO cells, transfection of the full-length E-cadherin resulted in growth stimulation by *Fn* (Figure 1D). As in HCT116, such stimulation was diminished by EC5 and the inhibitory peptide (Figure 1D). Similar observations were made using purified FadAc instead of *Fn* (Figure S1). These results elucidate the critical role of E-cadherin in promoting *Fn*-driven CRC cell growth.

FadAc Activates E-Cadherin-Mediated Cellular Signaling

To investigate the downstream events subsequent to FadA binding to E-cadherin, HCT116 cells were fractionated following incubation with purified FadA. FadAc, but not mFadA, bound to the HCT116 membranes within 5 min of incubation, leading to

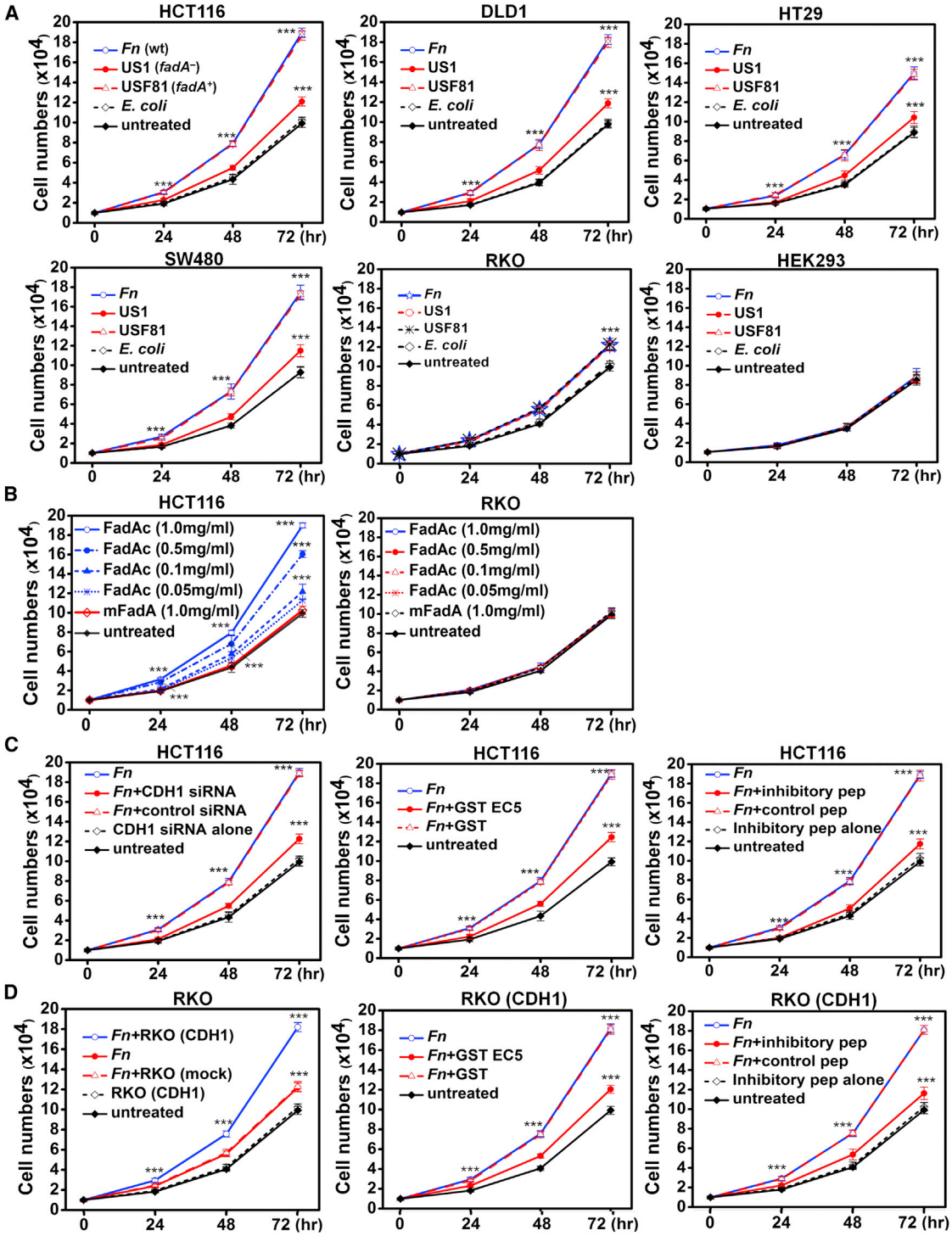

Figure 1. *Fn* and FadA Stimulate Proliferation of Human Colon Cancer Cells via E-Cadherin

(A) Wild-type *Fn* (*Fn*) and the *fadA*-complementing USF81 (*fadA*$^+$) stimulated proliferation of human CRC cells HCT116, DLD1, SW480, and HT29, compared to untreated cells or those incubated with *E. coli*. US1 (*fadA*$^-$) only weakly stimulated their growth. *Fn*, USF81, and US1 all weakly stimulated the growth of CRC RKO cells, but not the noncancerous HEK 293 cells.

(B) Purified FadAc stimulated HCT116 cell growth in a dose-dependent manner, while mFadA did not. Neither FadAc nor mFadA stimulated RKO cell growth.

(C) Suppression of *Fn*-stimulated cell growth by inhibiting E-cadherin. *Fn*-stimulated HCT116 growth was inhibited by siRNA specific for CDH1, GST-EC5 fusion protein, and the inhibitory peptide (IP), but not by nonspecific siRNA, GST, or the control peptide (CP).

(D) *Fn* stimulated the growth of RKO cells transfected with CDH1, but not mock-transfected RKO. Growth stimulation of CDH1-transfected RKO cells was suppressed by GST-EC5 and the inhibitory peptide, but not by GST or the control peptide. The results are presented as mean ± SD. ***$p < 0.001$. See also Figure S1.

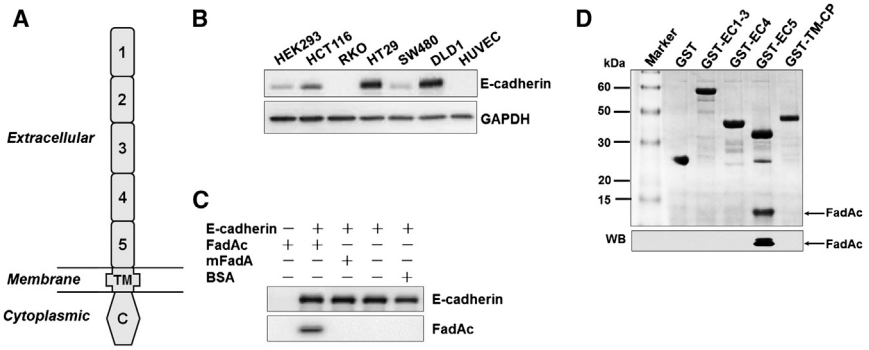

Figure 2. E-Cadherin Is a FadA Receptor

(A) Schematic representation of the E-cadherin (CDH1) structure. E-cadherin has five extracellular cadherin (EC) repeats, numbered EC1–EC5 starting from the N terminus. TM, transmembrane domain; C, cytoplasmic domain.

(B) E-cadherin is expressed in epithelial HEK 293 cells and most CRC cells. E-cadherin in HEK 293 and human CRC cell lines HCT116, RKO, HT29, SW480, and DLD1 was examined by western blot. Human umbilical vein endothelial cells (HUVECs) were included as a negative control. The endogenous GAPDH was used as a loading control.

(C) E-cadherin coimmunoprecipitates with FadAc. HEK 293 cell lysate expressing E-cadherin was mixed with *E. coli* lysates expressing FadAc or mFadA, or BSA, followed by incubation with mouse anti-CDH1 monoclonal antibodies (mAb), and captured with protein A/G agarose beads. E-cadherin and FadA in the bead elutes were detected by western blot.

(D) FadA binds to EC5. Purified GST or GST fusion proteins carrying EC1–EC3, EC4, or EC5 were incubated with *E. coli* lysates expressing FadAc, followed by capture with GST resin. The eluted components were subjected to SDS-PAGE, followed by Coomassie blue staining (top panel) and western blot (WB) using anti-FadA mAb 5G11-3G8 (bottom panel). See also Figure S2.

E-cadherin phosphorylation on the membrane and internalization (Figure 5A). This was accompanied by decreased phosphorylation of β-catenin, β-catenin accumulation in the cytoplasma, and translocation into the nucleus, resulting in activation of β-catenin-regulated transcription (CRT), as evidenced by increased expression of transcription factors lymphoid enhancer factor (LEF)/T cell factor (TCF), NF-κB, and oncogenes Myc and cyclin D1 (Figure 5A). It was previously shown that protein tyrosine kinase (PTK) plays a crucial role in E-cadherin endocytosis and recycling (Le et al., 2002). Interestingly, the PTK inhibitor genistein not only prevented E-cadherin phosphorylation and internalization, but also abolished FadA binding to the membranes and its internalization as well as the above-described CRT activation (Figure 5A). These results suggest that phosphorylation of E-cadherin or other cellular components are required for activation of CRT. FadA may bind to phosphorylated E-cadherin, or it may bind to nonphosphorylated E-cadherin, which is then phosphorylated, leading to positive feedback. The central role of β-catenin in regulating the cellular responses was confirmed using HCT116 β-catenin$^{-/-}$ cells, which did not affect FadA binding to E-cadherin, phosphorylation of E-cadherin, or its internalization, but prevented all gene activations tested in the nuclei (Figure 5A).

Although it did not affect FadA binding to E-cadherin or E-cadherin phosphorylation on the membranes, the clathrin inhibitor inhibited FadA and E-cadherin internalization. A surprise consequence was the divergent responses observed in the nuclei. Translocation of β-catenin and expression of LEF/TCF, Wnt, and oncogenes were unaffected. In contrast, no NF-κB activation was observed (Figure 5A). These results indicate that tumor growth and inflammatory responses, although both requiring β-catenin, are differentially regulated.

The western blot analysis of protein levels was corroborated with real-time quantitative PCR (qPCR) analysis of the messenger RNA (mRNA) levels (Figures 5B–5E). While the PTK inhibitor and CDH1-specific siRNA inhibited activation of tumor growth and inflammatory genes, the clathrin inhibitor only inhibited the inflammatory genes, but not the Wnt or oncogenes.

To further confirm the role of FadA in CRT activation, we performed confocal microscopy analysis and observed nuclei translocation of β-catenin in HCT116 in response to wild-type *Fn*, but not to US1 (*fadA*$^{-}$) (Figure 5F). In addition, wild-type *Fn* and USF81 (*fadA*$^{+}$), but not US1 (*fadA*$^{-}$), activated the luciferase reporter gene in TOPFlash carrying the β-catenin response promoter, but not in FOPFlash carrying the β-catenin nonresponse promoter (Figure 5G).

FadA Promotes E-Cadherin-Mediated CRC Tumor Growth and Induction of Proinflammatory Cytokines in Xenograft Mice

To examine the effects of FadA and *Fn* on CRC cell growth in vivo, HCT116 cells were inoculated into nude mice, followed by treatment with either purified protein or bacteria. Tumor growth was increased by 20% after 3 weeks of treatment by FadAc, compared to those treated with mFadA or BSA (Figures 6A and 6D). No increase was detected in the presence of 0.01 μmol inhibitory peptide, indicating the role of FadA binding to E-cadherin in tumor growth (Figures 6B and 6D). FadAc had no stimulatory effect on the non-E-cadherin-expressing RKO (Figure 6C).

When wild-type *Fn* was injected into HCT116 xenografts, abscess formation was observed within 3–5 days (data not shown). Immunohistochemical analysis using anti-*Fn* antibodies showed that wild-type *Fn* invaded the tumor tissues, while neither US1 (*fadA*$^{-}$) (Figure 6E) nor *E. coli* DH5α did (data not shown). *Fn* invasion was prevented by the inhibitory peptide, but not by the control peptide (Figure 6E). FadAc (Figure S4) and wild-type *Fn* (Figure 6F) stimulated the tumor growth genes and the inflammatory genes to same extent, which were inhibited by the inhibitory peptide, but not the control peptide, consistent with the observations in vitro.

Patients with CRC and Precancerous Adenomas Have Elevated *fadA* Gene and Expression Levels Compared to Normal Individuals

We examined *fadA* gene and expression levels in human colon specimens from the following five groups: (1) normal, noncancerous individuals (n = 14); (2) normal tissues from patients with precancerous adenomas (n = 16); (3) precancerous adenomas (n = 16); (4) normal tissues from patients with

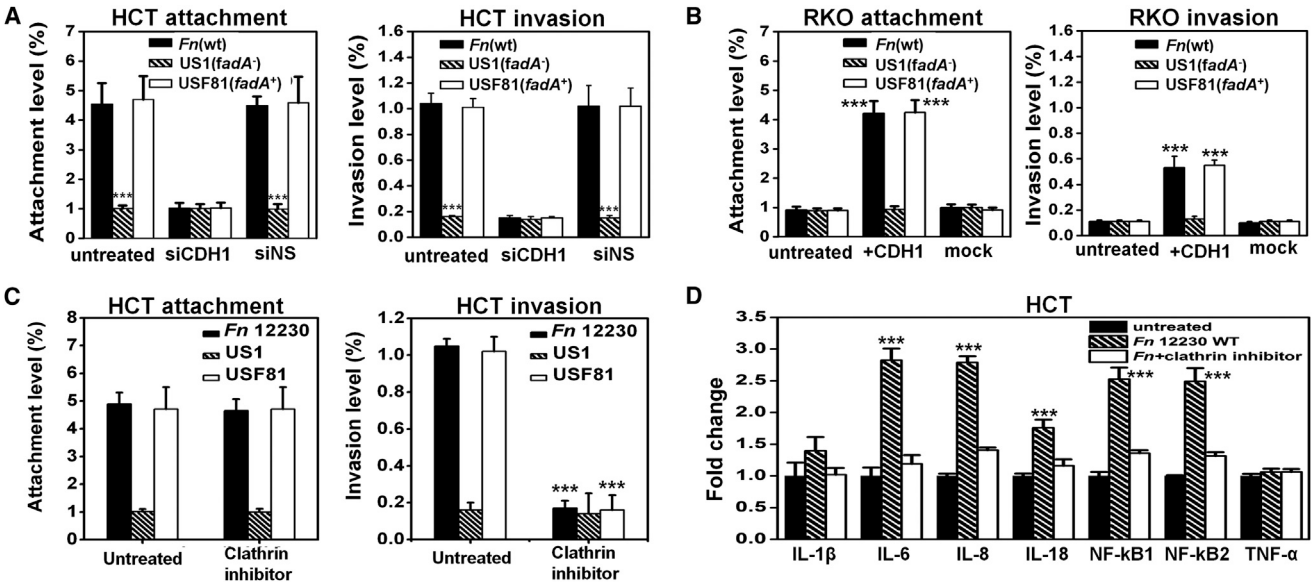

Figure 3. *Fn* Adheres to and Invades E-Cadherin-Expressing CRC Cells

(A) *Fn* adheres to and invades the E-cadherin-expressing HCT116 via FadA and E-cadherin. The *fadA*-deletion mutant US1 (*fadA*$^-$) was defective for attachment and invasion, compared to wild-type *Fn* and the *fadA*-complementing clone USF81 (*fadA*$^+$). Transfection with siRNA to inhibit E-cadherin expression (siCDH1) reduced attachment and invasion, while the nonspecific siRNA (siNS) did not.

(B) Wild-type *Fn*, US1, and USF81 were defective for attachment and invasion of the non-E-cadherin-expressing RKO cells. Transfection of full-length CDH1 into RKO enhanced attachment and invasion by wild-type *Fn* and USF81 (*fadA*$^+$), but not by US1 (*fadA*$^-$).

(C) The clathrin inhibitor, Pitstop2, inhibits *Fn* and USF81 (*fadA*$^+$) invasion of HCT116 without affecting their attachment.

(D) Wild-type *Fn* stimulates expression of NF-κB and proinflammatory cytokines IL-6, IL-8, and IL-18 in HCT116, which was inhibited by the clathrin inhibitor. Expression levels in untreated HCT116 were designated as 1. For (A), (B), and (D), the attachment and invasion levels were expressed as percent of bacteria recovered from the host cells relative to the initial inoculum. For wild-type *Fn*, these levels reflect recovering approximately 9,000 cfu per well (in a 96-well plate) from the attachment assay and approximately 2,000 cfu per well from the invasion assay. The invasion level of *E. coli* DH5α into HCT116 was <0.01%, i.e., <20 cfu recovered per well (data not shown). For (C), the original attachment (4.4% ± 0.8%) and invasion (1.3% ± 0.1%) levels without inhibition were designated as 100%, and the relative inhibition values were shown. The results are presented as the mean ± SD. ***$p < 0.001$. See also Figure S3.

adenocarcinomas (n = 19); and (5) adenocarcinomas (n = 19). A stepwise increase of *fadA* gene copies was observed from group 1 to groups 2–4 and from groups 2–4 to group 5, with >1 log difference between each step (Figure 7A). The biggest difference was observed between the noncancerous controls and CRC, with a >2 log difference (Figure 7A). Similar observations were made when *Fn*-specific 16S ribosomal RNA (rRNA) gene copies were measured (data not shown). The FadA mRNA levels in the colon tissues, when normalized to glyceraldehyde 3-phosphate dehydrogenase (GAPDH), also showed a stepwise increase correlating with the *fadA* gene copy numbers (data not shown). When the *fadA* mRNA levels were normalized to *Fn* 16S RNA to reflect *fadA* expression in *Fn*, a significant increase was only observed in the carcinoma tissues (Group 5), indicating that *Fn* exhibits increased virulence in CRC compared to the normal and precancerous tissues (Figure 7B). Consistent with the increase of *fadA*, expression of a representative Wnt gene, Wnt7b, and a representative inflammatory gene, NFkB2, was also significantly increased in CRC, corroborating with the results obtained in vitro and in xenograft mice (Figures 7C and 7D).

DISCUSSION

CRC is the second leading cause of cancer death in men and women combined in the US. (ACS, 2012). Worldwide, over one million new cases are diagnosed each year (Bartlett and Chu, 2012). Understanding the mechanisms of CRC and identifying risk factors are important to human health. Increasing evidence supports a relationship between infective agents and various human malignancies (Plottel and Blaser, 2011). Previous studies have provided mechanistic insights into the microbial involvement in the development of CRC (Arthur et al., 2012; Cuevas-Ramos et al., 2010; Lee et al., 2010; Wu et al., 2009). It was reported that *Bacteroides fragilis* enterotoxin BFT cleaves E-cadherin to activate β-catenin signaling (Wu et al., 1998; 2003). Here, we report a mechanism by which *Fn* modulates E-cadherin/β-catenin signaling.

Fn significantly stimulates proliferation of E-cadherin-expressing CRC cells, but not those without E-cadherin. The stimulation requires FadA, an E-cadherin ligand. The *fadA*-deletion mutant US1 has weak stimulatory activity. These observations indicate that the interactions between FadA and E-cadherin play a primary role in promoting CRC tumor growth, while the FadA-independent pathway(s) play a minor role.

E-cadherin is a tumor suppressor that functions through β-catenin (Bryant and Stow, 2004; Peifer and Polakis, 2000). It has been previously reported that E-cadherin is present in 100% of the normal mucosa of CRC patients and 75% of cancer specimens (Mohri, 1997). Loss or heterogeneous expression of E-cadherin correlated with advanced stages of CRC and poor prognosis (Mohri, 1997; Dorudi et al., 1993). FadA binding to

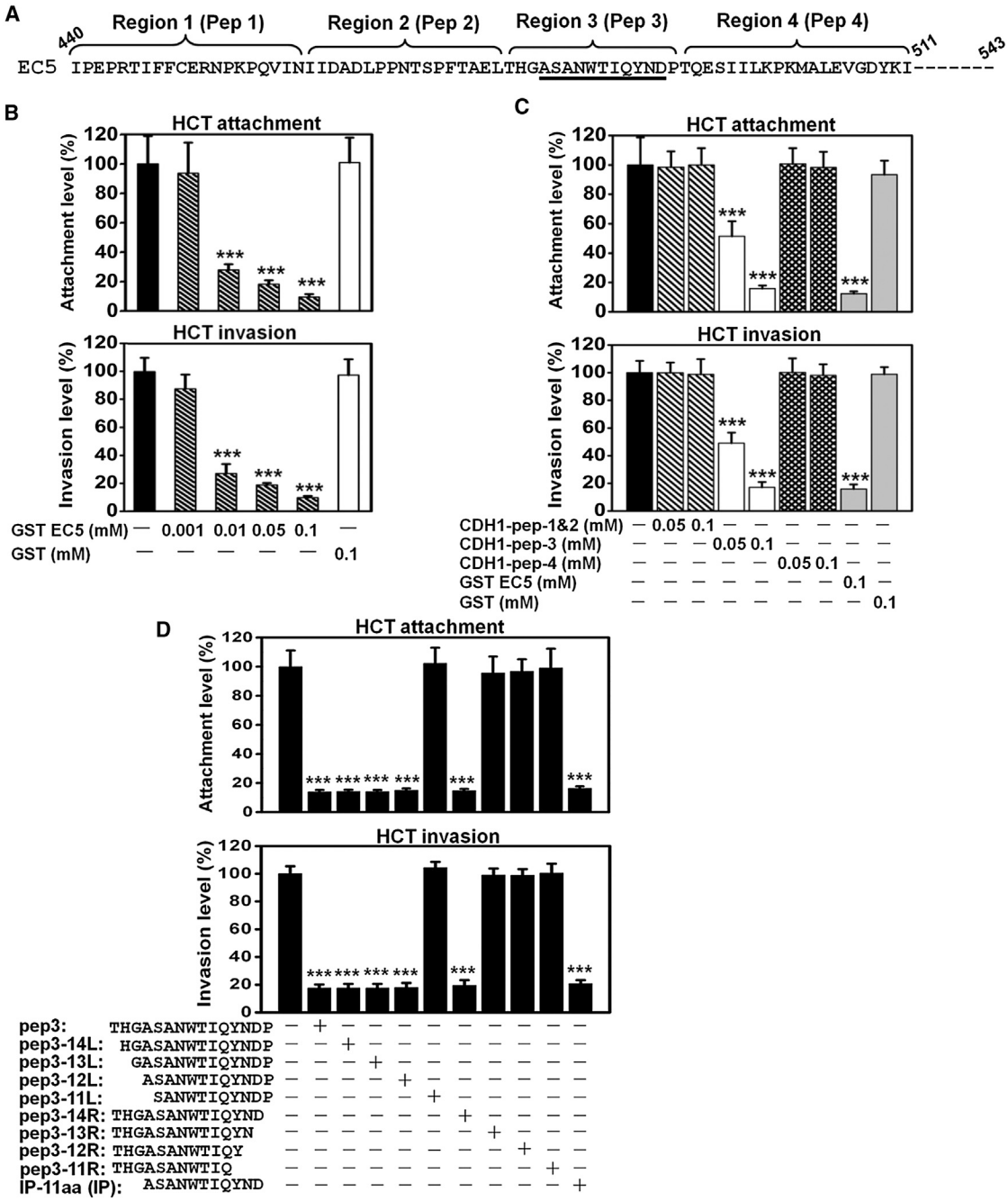

Figure 4. Identification of Synthetic Peptides to Inhibit *Fn* Attachment and Invasion of HCT116 Cells

(A) Partial amino acid sequence of the EC5 domain. The regions and the corresponding peptides (pep) are shown above the sequence. The sequences corresponding to the inhibitory peptide (IP, see below) are underlined. Peptide 4 was the control peptide (CP) in all studies.

(B) Purified GST-EC5 fusion protein inhibits wild-type *Fn* attachment and invasion of HCT116 in a dose-dependent manner.

(C) *Fn* attachment and invasion of HCT116 cells were inhibited by a synthetic peptide corresponding to region 3 (pep 3) on the EC5 domain, not by peptides corresponding to regions1 and 2 or 4.

(D) The inhibitory effects of synthetic oligopeptides carrying sequential deletions from the N and C termini of region 3 on *Fn* attachment and invasion. Deletion of 3 residues from the N terminus and 1 residue from the C terminus did not affect the inhibitory function. An 11 aa peptide (ASANWTIQYND) was found as the minimum sequence required for inhibition of *Fn* attachment and invasion. All values were expressed relative to those without inhibition, which were designated as 100%. The actual attachment and invasion levels were 6.3% ± 1.4% and 1.6% ± 0.1%, respectively, for (B); 5.9% ± 0.7% and 1.4% ± 0.1%, respectively, for (C); and 5.3 ± 0.5% and 1.3 ± 0.1%, respectively, for (D). The results are presented as mean ± SD. ***p < 0.001.

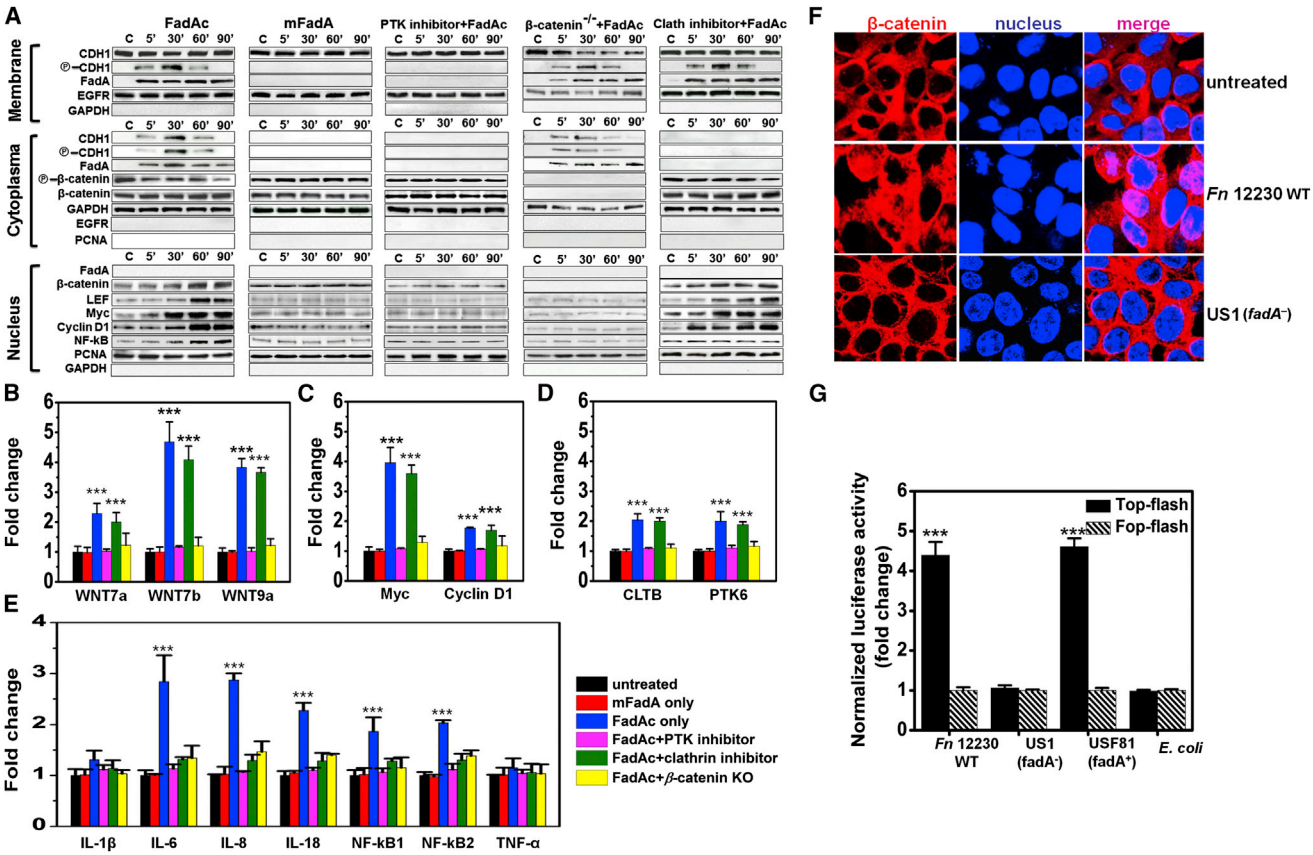

Figure 5. FadAc Activates E-Cadherin-Mediated Cellular Signaling

(A) Western blotting was used to detect the following: (1) FadAc, but not mFadA, binds to the membranes of HCT116, accompanied by phosphorylation of E-cadherin on the membrane; (2) E-cadherin and FadA are internalized, phosphorylation of β-catenin is reduced, and total β-catenin accumulates in the cytoplasma; and β-catenin translocates and transcription factors lymphoid enhancer factor (LEF)/T cell factor (TCF), NF-κB, and oncogenes Myc and cyclin D1 are activated in the nuclei. Protein tyrosine kinase (PTK) inhibitor genistein inhibits all FadAc-activated functions. No gene activation was detected in the HCT116 β-catenin$^{-/-}$ cells, despite binding and internalization of FadA and E-cadherin. The clathrin inhibitor Pitstop2 prevented E-cadherin and FadA internalization and activation of NF-κB, but did not affect nuclei translocation of β-catenin or expression of LEF/TCF, Myc or cyclin D1. The epidermal growth factor receptor (EGFR), GAPDH, and proliferating cell nuclear antigen (PCNA) were used as loading controls for membrane, cytoplasmic, and nucleus, respectively, and for examination for cross-contamination between the subcellular fractions.

(B–E) FadAc, but not mFadA or BSA, activates expression of Wnt signaling genes 7a, 7b, and 9a (B); oncogenes Myc and cyclin D1 (C); clathrin (cltb) and protein tyrosine kinase genes (ptk6) (D); and NF-κB and proinflammatory cytokines IL-6, IL-8, and IL-18 (E) in wild-type, but not in β-catenin knockout HCT116 cells following 2 hr incubation as determined by qPCR. The clathrin inhibitor inhibited expression of the inflammatory genes, but not the Wnt or oncogenes. Expression levels in untreated HCT116 cells were designated as 1.

(F) Wild-type *Fn* (*Fn*), but not US1 (*fadA*$^{-}$), induces nuclei translocation of β-catenin following 2 hr incubation, as observed by confocal microscopy. β-catenin was stained with Alexa 634 (red) and the nuclei with DAPI (blue). The purple color in the merged images indicates translocation of β-catenin into the nuclei.

(G) Luciferase reporter gene expression following HCT116 transfection with TOPFlash (activated by β-catenin) or FOPFlash (insensitive to β-catenin activation). *Fn* was incubated with the transfected cells at an moi of 1,000:1 for 2 hr, followed by measurement of the luciferase activity. Values obtained with FOPFlash were designated as 1, and those obtained with TOPFlash were expressed as fold changes. Data are presented as mean fold changes ± SD of two independent experiments, each performed in triplicate. ***$p < 0.001$.

E-cadherin inhibits its tumor suppressor activity, resulting in increased CRT. This phenotype is consistent with the adenomatous polyposis coli (APC) mutation, the most common mutation in CRC (Kinzler and Vogelstein, 2002). The four human colon cancer cell lines stimulated by FadA, HCT116, DLD1, SW480, and HT29, carry either an APC mutation (DLD1, SW480, and HT29) (Yang et al., 2006) or a β-catenin mutation (HCT116) (Morin et al., 1997), and thus have increased CRT background (Chan et al., 2002). FadA, both in purified form and in *Fn*, further enhanced CRT and stimulated the growth of these cells, attesting to its carcinogenic potency. Interestingly, FadA does not stimulate the growth of the noncancerous HEK 293, suggesting that it promotes carcinogenesis after a mutation occurs.

FadA is the major component mediating *Fn* attachment and invasion (Xu et al., 2007). It binds to an 11 aa region in the EC5 domain on E-cadherin and is internalized with E-cadherin. The 11 aa inhibitory peptide inhibits *Fn* from binding and invading and abolishes all subsequent host responses, including tumor growth and inflammatory responses. Thus, this inhibitory peptide not only prevents *Fn* colonization but also inhibits *Fn*-mediated oncogenesis.

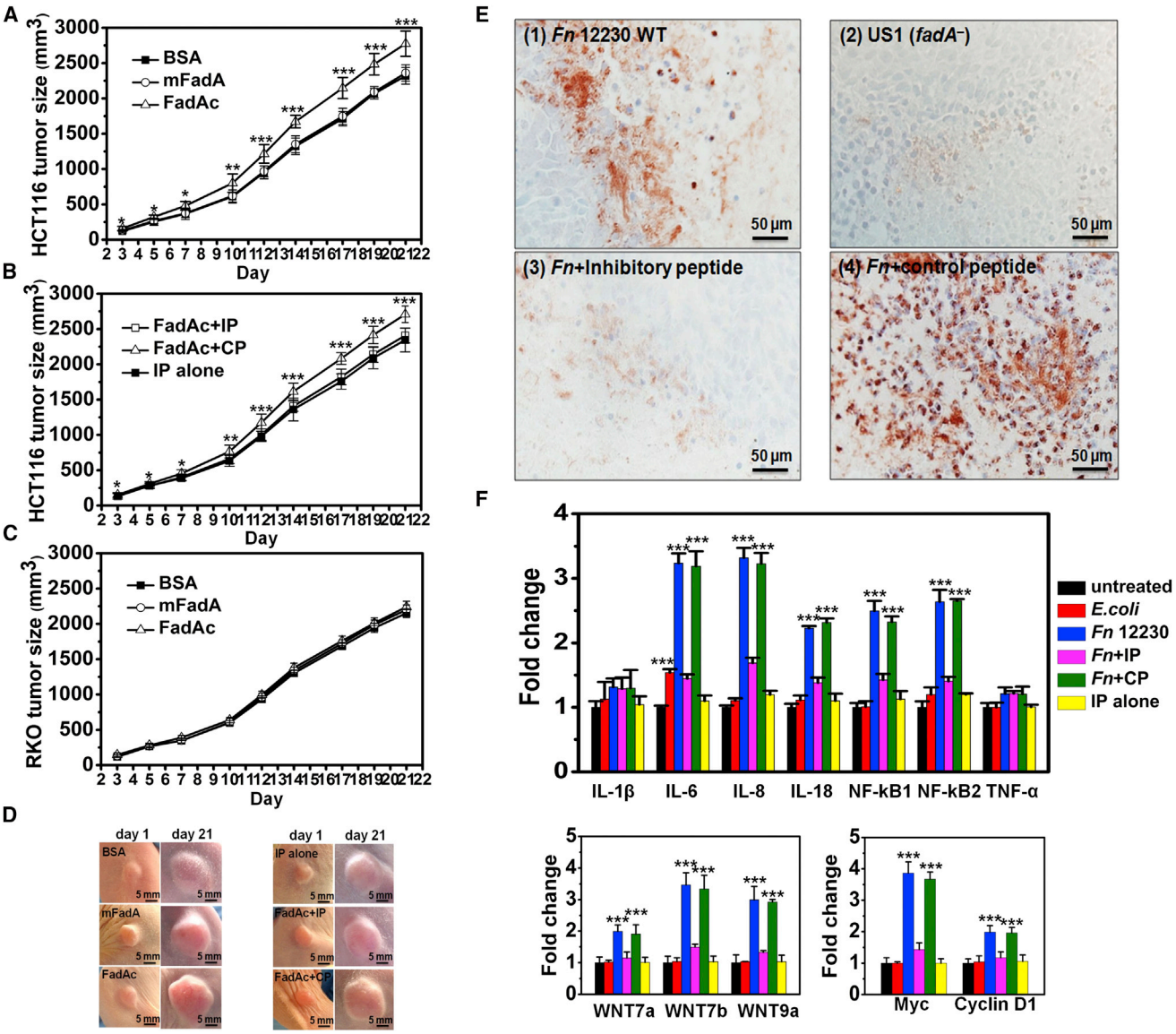

Figure 6. FadA Promotes E-Cadherin-Mediated CRC Tumor Growth and Induction of Proinflammatory Cytokines in Xenograft Mice

HCT116 or RKO cells were injected subcutaneously and bilaterally into female nude mice, which were then randomized (five per group) to receive treatments. (A–C) FadAc stimulates HCT116, but not RKO, xenograft growth. Purified FadAc, mFadA, or BSA were injected into xenografts of HCT116 either alone (A) or along with the inhibitory (IP) or control (CP) peptides (B) or RKO alone (C) in nude mice. IP alone is injected into HCT116 as a negative control (B).

(D) Representative tumors from (A) and (B) are shown. The first day of protein injection was designated as day 1. All tumors look the same on day 1. Notice the size increase of the tumor treated with FadAc and FadAc + CP on day 21 compared to other tumors on the same day.

(E) Immunohistochemical staining of xenografts infected with wild-type *Fn* (*Fn*), alone and with the inhibitory or control peptides, and the *fadA*-deletion mutant US1 (*fadA*$^-$) using rabbit anti-*Fn* polyclonal antibodies. For controls, xenografts infected with wild-type *Fn* were stained with pre-serum, and xenografts infected with *E. coli* DH5α were stained with anti-*Fn* antibodies (data not shown).

(F) Wild-type *Fn* induces expression of NF-κB and proinflammatory cytokines IL-6, IL-8, and IL-18; Wnt 7a, 7b, and 9a; and Myc and cyclin D1 in HCT116 xenografts, as determined by qPCR. The inductions were inhibited by IP, but not by CP. *E. coli* only weakly induced IL-6. The results are presented as mean ± SD. ***$p < 0.001$. See also Figure S4.

Inflammation plays a key role in CRC oncogenesis (Baron and Sandler, 2000; Ekbom et al., 1990). In this issue, Kostic et al. (2013) showed that *Fn* generates a proinflammatory microenvironment that is conducive for colorectal neoplasia progression (Kostic et al., 2013). Both the observations herein and by Kostic et al. (2013) support that inflammatory stimulation by *Fn* further reinforces the oncogenic potential of this microorganism. As shown in the xenografts, FadA alone was able to stimulate the inflammatory responses to the same extent as *Fn*, indicating that FadA is the major stimulant of inflammation.

Our results reveal that tumor growth and inflammation are differentially regulated, although both require β-catenin, the

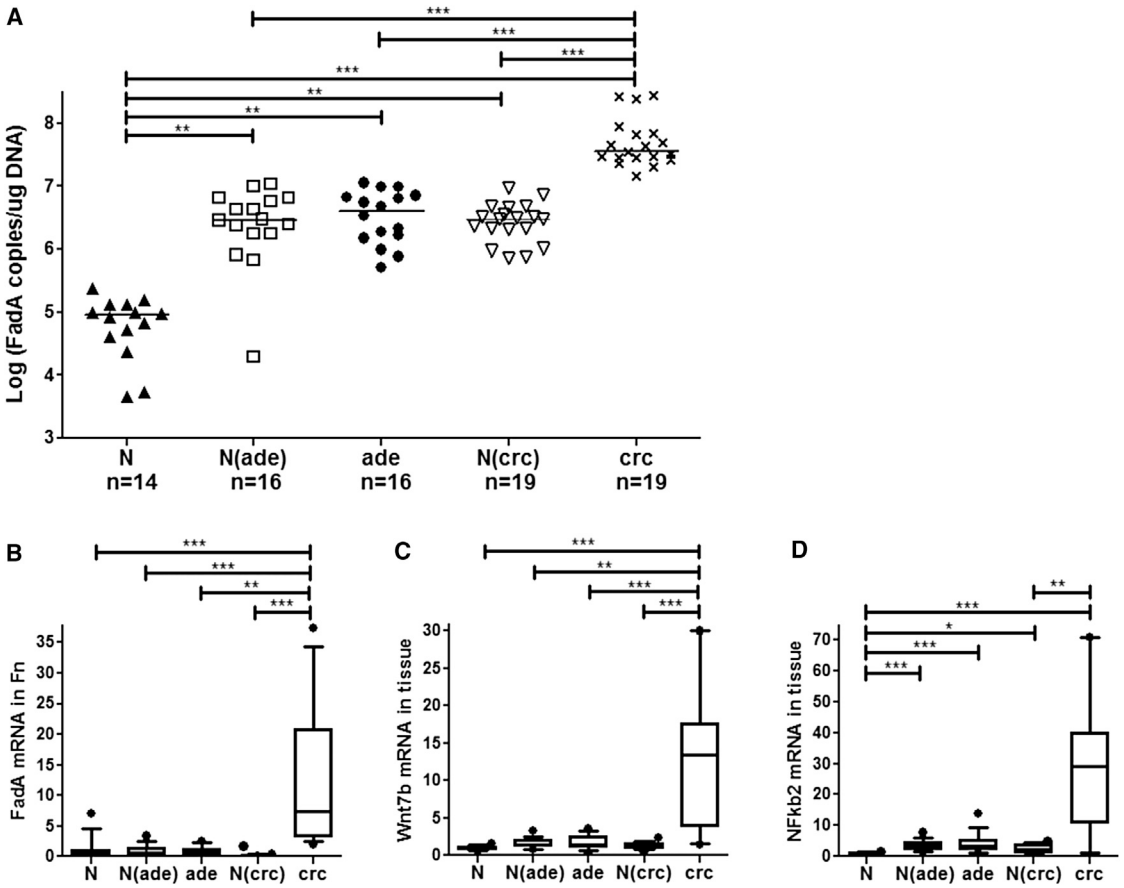

Figure 7. Quantification of *fadA* Gene Copies and FadA, Wnt7b, and NFkB2 Expression in Healthy Cells, Precancerous Adenomas, and Carcinomas

(A–D) DNA and RNA were extracted from full-thickness colon specimens from the following 5 groups: (1) normal, noncancerous controls (N; n = 14); (2) normal tissues from patients with precancerous adenomas (N[ade]; n = 16); (3) precancerous adenomas (ade; n = 16); (4) normal tissues from patients with carcinomas (N [crc]; n = 19); and (5) carcinomas (crc; n = 19). Gene copy numbers of *fadA* (A) were measured using DNA and determined using the standard curves. FadA mRNA levels in *Fn* were normalized to *Fn* 16 rRNA (B), and Wnt7b (C) and NFkB2 (D) mRNA levels were each normalized to the endogenous GAPDH. The average value of group 1 (N) was designated as 1, and the fold changes of the other groups were determined by comparing to group 1. The horizontal bars represent the median values. For (B)–(D), the boxes show the 25th and 75th percentiles and the lines within the boxes the median values. Whiskers show the 10th and 90th percentiles. *p < 0.05, **p < 0.01, and ***p < 0.001.

master regulator. It is often difficult to distinguish the roles of adherence and invasion, as these two processes are tightly correlated (Martin et al., 2004; Swidsinski et al., 1998), with the former being a prerequisite for the latter. Using the clathrin inhibitor, we are able to functionally separate *Fn* attachment from invasion and demonstrate that although invasion is not required for tumor growth, it is essential for the induction of inflammation, which is consistent with a previous report that the invasive potential of *Fn* correlates with the host inflammatory bowel disease (IBD) status (Strauss et al., 2011).

The mechanistic investigation is corroborated with studies in humans. Previous studies have shown that *Fn* is readily detected in the tissues, but not in the stools (Chen et al., 2012). This may be due to its adherent and invasive properties. Hence, we examined the presence of *Fn* in colon tissue specimens, rather than stools. The results unveil a stepwise increase of *fadA* gene copies from the baseline of normal individuals to adenomas and normal tissues adjacent to adenomas and adenocarcinomas and to adenocarcinomas. The normal tissues from patients with adenomas and adenocarcinomas are thus "pseudonormal" compared to the noncancerous controls. This is consistent with the findings by McCoy et al. (2013). Given the fact that FadA mediates *Fn* binding to both CRC and non-CRC cells, and the fact that the normal tissues also express E-cadherin, it is not surprising that *Fn* can colonize both tumor and nontumor sites. Elevated *Fn* colonization in the normal tissues may predispose the host to the development of adenomas and/or adenocarcinoma, with carcinogenesis being accelerated when a mutation occurs. The fact that FadA expression levels in *Fn*, as well as the host inflammatory and oncogenic responses, are increased in the cancerous tissues, but not in the precancerous tissues, further supports this notion.

The finding of elevated *fadA* levels in the precancerous state implies translational potential. Compared to the metagenomic approach in the previous studies (Castellarin et al., 2012; Kostic et al., 2012), qPCR is significantly less time consuming and more

cost effective, which is suitable for clinical purposes. The *fadA* gene is unique to *Fn* (Han et al., 2005) and, hence, is an ideal potential diagnostic marker to identify individuals at risk for developing adenomas and/or adenocarcinomas. Based on the results shown in Figure 7, it is possible that diagnostic criteria may be developed to define healthy, precancerous, and cancerous states according to *fadA* gene copy levels. One limitation of the current study is the small sample size. The potential use of *fadA* as a diagnostic marker needs to be evaluated in a much larger prospective cohort. Future studies are also warranted to examine the use of the inhibitory peptide and/or its derivatives to eradicate *Fn*, either as a preventive therapy for individuals with increased risk or as a complementary therapy for those with CRC.

In conclusion, we have elucidated an oncogenic mechanism of CRC. Findings from this study will significantly impact our understanding, diagnosis, prevention, and treatment of CRC.

EXPERIMENTAL PROCEDURES

Bacterial Strains, Cell Cultures, Construction of Plasmids, Protein Purification, and GST Pull-Down Assays

Bacteria and human cell lines were cultured as previously described (Fardini et al., 2011; Han, 2006; Zhang et al., 2013). Extracellular (EC) domains of E-cadherin were amplified by PCR from pcDNA3-E-cadherin (Addgene) vector using primers listed in Table S1. Protein expression and purification as well as GST pull-down assays were all performed as previously described (Fardini et al., 2011; Xu et al., 2007).

Tissue Culture Attachment and Invasion Assays

These assays were performed as previously described (Han et al., 2000). Briefly, cells were seeded in 24-well or 96-well plates at 8×10^4 cells or 2.5×10^4 cells per well in the growth medium and grown to 100% confluency. Bacteria were added to the cells at a multiplicity of infection (moi) of 5. Following 1 hr incubation at 37°C in 5% CO_2, the monolayers were washed 3 times with Dulbecco's phosphate-buffered saline (DPBS) (pH 7.1) supplemented with Ca^{2+} and Mg^{2+}. Cells were lysed with water for 20 min at 37°C. Serial dilutions of the lysates were plated onto blood agar plates to enumerate the total cell-associated bacteria. For invasion assays, the bacteria were incubated with the monolayers at 37°C for 4 hr, followed by washes with PBS. Fresh media containing 300 μg/ml gentamicin and 200 μg/ml metronidazole were added to the monolayers and incubated for an additional hour to kill extracellular bacteria. The cells were then washed and lysed with water as described above. The levels of attachment and invasion were expressed as the percentage of bacteria recovered following cell lysis relative to the total number of bacteria initially added. Each experiment was performed in triplicate and repeated at least twice.

Antibodies, Peptides, and Western Blot Analysis

The following antibodies were used: anti-FadA monoclonal antibody (mAb) 5G11-3G8 (Xu et al., 2007), mAb anti-CDH1 (Abcam or Cell Signaling Technology), polyclonal anti-phospho-CDH1 (ECM Biosciences), mAb anti-GAPDH (Invitrogen), mAb anti-β-catenin (R&D Systems), polyclonal anti-phospho-β-catenin (Cell Signaling Technology), mAb anti-LEF/TCF1 (Invitrogen), mAb anti-NF-κB (Invitrogen), mAb anti-Myc (Cell Signaling Technology), mAb anti-cyclin D1 (Cell Signaling Technology), mAb anti-EGFR (Cell Signaling Technology), mAb anti-GAPDH (Cell Signaling Technology), mAb anti-PCNA (Cell Signaling Technology), polyclonal goat anti-mouse or goat anti-rabbit secondary antibody conjugated with horseradish peroxidase (HRP) (Pierce Biotechnology). Peptides were synthesized by NEO Group Inc. Western blot analyses were performed as previously described (Fardini et al., 2011).

Coimmunoprecipitation Assay

A total of 500 μg of HEK 293 cell lysate prepared with Co-IP Lysis/Wash Buffer (Pierce) was mixed with 100 μg of BSA or *E. coli* lysate expressing FadAc or mFadA, followed by the addition of mouse monoclonal anti-CDH1 antibodies. The protein complex was captured by protein A/G agarose beads (Santa Cruz) as previously described (Chan et al., 2002), followed by elution and western blot analysis. An equal volume of the eluted components was loaded onto SDS-PAGE.

DNA and siRNA Transfection

CDH1 transfections were performed as previously described (Lebreton et al., 2011). siRNA assays were performed using the FlexiTube siRNA anti-CDH1 reagent and AllStars FlexiTube Control siRNA from QIAGEN according to the manufacturer's instructions.

Cell Proliferation Assay

CRC cells were seeded in 24-well plates at 1×10^4 cells per well in the growth medium. Cells were untreated or incubated with FadAc or peptides at the indicated concentration or with bacteria at an moi of 1000:1. Cell numbers were counted at 24 hr intervals using a hemocytometer. Each experiment was performed in triplicate and repeated at least twice.

Preparation of Subcellular Fractions

Cells were incubated with 1 mg/ml of FadAc or mFadA followed by the extraction of subcellular fractions. When indicated, 50 μM of the corresponding PTK inhibitor (genistein) and clathrin inhibitor (Pitstop2) were preincubated with cells for 1 hr. Membrane, cytosolic, and nuclei fractions were prepared using the Compartmental Protein Extraction Kit (Millipore) according to the manufacturer's instructions.

Luciferase Reporter Assay

HCT116 cells were seeded in 96-well plates at 2.5×10^4 cells per well in the growth medium and grown to 100% confluency. Cells were transfected with 0.2 μg of TOPFlash, a luciferase reporter vector carrying TCF promoter upstream of the luciferase gene and able to be activated by β-catenin, or FOPFlash (with mutations rendering insensitivity to β-catenin activation), using Lipofectamine 2000 (Invitrogen) according to the manufacturer's instructions. On the following day, cells were incubated with bacteria at an moi of 1000:1 for 2 hr. Reporter assays were performed using the luciferase reporter system (Promega). The experiment was performed in triplicate and repeated twice.

Immunofluorescent and Immunohistochemical Staining

Immunofluorescent staining of cells was performed as previously described. Mouse anti-β-catenin mAb and Alexa Fluor 634-conjugated goat anti-mouse polyclonal antibodies were used (Fardini et al., 2011). Immunohistochemical (IHC) analysis of xenograft tumors was performed as previously described, using rabbit anti-*Fn* polyclonal antibodies (Han et al., 2004). Preimmune serum from the same rabbit was used as control.

Xenografts

The animal protocol was approved by the Case Western Reserve University Institutional Animal Care and Use Committee. An inoculum of 5×10^6 cells were injected subcutaneously (s.c.) and bilaterally into 4- to 6-week-old female nude mice (5 per group) as previously described (Zhang et al., 2013). The mice were randomized to receive one of the following: FadAc or mFadA (each at 80 μg) with or without peptide (0.01 μmol), BSA (0.01 μmol, i.e., 660 μg), or bacteria at 1×10^7 colony-forming units (cfu) at each inoculation site. Xenograft volumes were calculated as previously described (Zhang et al., 2013).

Clinical Specimens

This study was approved by the University Hospitals of Cleveland Institutional Review Board. A total of 19 cases diagnosed with colonic adenocarcinoma and 16 cases of adenomas were retrieved from files at the Department of Pathology of the University Hospitals Case Medical Center. Hematoxylin and eosin (H&E) slides were reviewed to confirm the presence of adenocarcinoma (or adenoma). A representative block of colon adenocarcinoma (or adenoma) and a block of normal colon from the same patient were used. In addition, normal colon tissues were derived from 14 individuals undergoing resection for benign colon pathology or resection of adjacent organs. Exclusion criteria were history of gastrointestinal malignancies, presence of prominent inflammation or abscess, and history of IBD. All cases were from within the last

12 months. Genomic DNA was extracted from formalin-fixed paraffin-embedded tissue samples as previously described (Tang et al., 2009). RNA was extracted using PureLink FFPE Total RNA Isolation Kit (Invitrogen) or RNeasy FFPE Kit (QIAGEN).

Real-Time Quantitative PCR

Total RNA was extracted from CRC cells, xenografts, or clinical specimens. cDNA synthesis and real-time PCR were performed as previously described, using primers listed in Table S1 (Lebreton et al., 2011). Data were analyzed by the ΔΔCt method (Livak and Schmittgen, 2001) and normalized to the GAPDH or *Fn*-specific 16S rRNA. To quantify the *fadA* gene copies, plasmid carrying *fadA* was serially diluted to 10^2–10^8 *fadA* copies/μl and used to generate standard curves for Ct values. The *fadA* gene copies in the clinical samples were calculated based on the standard curves. Each experiment was performed in triplicate and repeated at least three times.

Statistical Analysis

The differences between groups were examined by two-tailed one-way ANOVA followed by Student-Newman-Keuls (SNK) test. For the clinical specimens, the Kruskal-Wallis nonparametric test was performed, followed by the Conover test. $p < 0.05$ was considered statistically significant.

SUPPLEMENTAL INFORMATION

Supplemental Information includes four figures and one table and can be found with this article online at http://dx.doi.org/10.1016/j.chom.2013.07.012.

ACKNOWLEDGMENTS

The authors declare no conflict of interest. We thank Zhenghe Wang for providing human cancer cell lines HCT116, DLD1, SW480, HT29, and RKO and helpful discussions, and Bert Vogelstein and Zhenghe Wang for providing the HCT116 β-catenin$^{-/-}$ cell line. This work was supported by the National Institute of Dental and Craniofacial Research grant RO1 DE14924 to Y.W.H. Y.W.H. conceived, designed, and supervised the study. W.L. provided clinical specimens. M.R.R., X.W., Y.H., and G.C. performed the experiments. Y.W.H., X.W., M.R.R., and W. L. interpreted the data and wrote the manuscript.

Received: February 25, 2013
Revised: June 14, 2013
Accepted: July 17, 2013
Published: August 14, 2013

REFERENCES

American Cancer Society. (2012). Cancer Facts & Figures 2012 (Atlanta: American Cancer Society), pp. 1–66.

Arthur, J.C., Perez-Chanona, E., Mühlbauer, M., Tomkovich, S., Uronis, J.M., Fan, T.J., Campbell, B.J., Abujamel, T., Dogan, B., Rogers, A.B., et al. (2012). Intestinal inflammation targets cancer-inducing activity of the microbiota. Science *338*, 120–123.

Baron, J.A., and Sandler, R.S. (2000). Nonsteroidal anti-inflammatory drugs and cancer prevention. Annu. Rev. Med. *51*, 511–523.

Bartlett, D.L., and Chu, E. (2012). Can metastatic colorectal cancer be cured? Oncology (Huntingt.) *26*, 266–275.

Bryant, D.M., and Stow, J.L. (2004). The ins and outs of E-cadherin trafficking. Trends Cell Biol. *14*, 427–434.

Castellarin, M., Warren, R.L., Freeman, J.D., Dreolini, L., Krzywinski, M., Strauss, J., Barnes, R., Watson, P., Allen-Vercoe, E., Moore, R.A., and Holt, R.A. (2012). Fusobacterium nucleatum infection is prevalent in human colorectal carcinoma. Genome Res. *22*, 299–306.

Chan, T.A., Wang, Z., Dang, L.H., Vogelstein, B., and Kinzler, K.W. (2002). Targeted inactivation of CTNNB1 reveals unexpected effects of beta-catenin mutation. Proc. Natl. Acad. Sci. USA *99*, 8265–8270.

Chen, W., Liu, F., Ling, Z., Tong, X., and Xiang, C. (2012). Human intestinal lumen and mucosa-associated microbiota in patients with colorectal cancer. PLoS ONE *7*, e39743.

Cuevas-Ramos, G., Petit, C.R., Marcq, I., Boury, M., Oswald, E., and Nougayrède, J.P. (2010). Escherichia coli induces DNA damage in vivo and triggers genomic instability in mammalian cells. Proc. Natl. Acad. Sci. USA *107*, 11537–11542.

Dorudi, S., Sheffield, J.P., Poulsom, R., Northover, J.M., and Hart, I.R. (1993). E-cadherin expression in colorectal cancer. An immunocytochemical and in situ hybridization study. Am. J. Pathol. *142*, 981–986.

Ekbom, A., Helmick, C., Zack, M., and Adami, H.O. (1990). Ulcerative colitis and colorectal cancer. A population-based study. N. Engl. J. Med. *323*, 1228–1233.

Fardini, Y., Wang, X., Témoin, S., Nithianantham, S., Lee, D., Shoham, M., and Han, Y.W. (2011). Fusobacterium nucleatum adhesin FadA binds vascular endothelial cadherin and alters endothelial integrity. Mol. Microbiol. *82*, 1468–1480.

Gumbiner, B.M. (2005). Regulation of cadherin-mediated adhesion in morphogenesis. Nat. Rev. Mol. Cell Biol. *6*, 622–634.

Han, Y.W. (2006). Laboratory maintenance of fusobacteria. In Current Protocols in Microbiology, R. Coico, T. Kowalik, J. Quarles, B. Stevenson, and R. Taylor, eds. (New York: John Wiley & Sons, Inc.).

Han, Y.W. (2011). Fusobacterium nucleatum interaction with host cells. In Oral Microbial Communities: Genomic Inquiry and Interspecies Communication, Chapter 15, P.E. Kolenbrander, ed. (Washington, D.C.: ASM Press).

Han, Y.W., Shi, W., Huang, G.T., Kinder Haake, S., Park, N.H., Kuramitsu, H., and Genco, R.J. (2000). Interactions between periodontal bacteria and human oral epithelial cells: Fusobacterium nucleatum adheres to and invades epithelial cells. Infect. Immun. *68*, 3140–3146.

Han, Y.W., Redline, R.W., Li, M., Yin, L., Hill, G.B., and McCormick, T.S. (2004). Fusobacterium nucleatum induces premature and term stillbirths in pregnant mice: implication of oral bacteria in preterm birth. Infect. Immun. *72*, 2272–2279.

Han, Y.W., Ikegami, A., Rajanna, C., Kawsar, H.I., Zhou, Y., Li, M., Sojar, H.T., Genco, R.J., Kuramitsu, H.K., and Deng, C.X. (2005). Identification and characterization of a novel adhesin unique to oral fusobacteria. J. Bacteriol. *187*, 5330–5340.

Han, Y.W., Shen, T., Chung, P., Buhimschi, I.A., and Buhimschi, C.S. (2009). Uncultivated bacteria as etiologic agents of intra-amniotic inflammation leading to preterm birth. J. Clin. Microbiol. *47*, 38–47.

Han, Y.W., Fardini, Y., Chen, C., Iacampo, K.G., Peraino, V.A., Shamonki, J.M., and Redline, R.W. (2010). Term stillbirth caused by oral Fusobacterium nucleatum. Obstet. Gynecol. *115*, 442–445.

Ikegami, A., Chung, P., and Han, Y.W. (2009). Complementation of the fadA mutation in Fusobacterium nucleatum demonstrates that the surface-exposed adhesin promotes cellular invasion and placental colonization. Infect. Immun. *77*, 3075–3079.

Kinzler, K.W., and Vogelstein, B. (2002). In The Genetic Basis of Human Cancer, B. Vogelstein and K.W. Kinzler, eds. (New York: McGraw–Hill), pp. 565–587.

Kostic, A.D., Gevers, D., Pedamallu, C.S., Michaud, M., Duke, F., Earl, A.M., Ojesina, A.I., Jung, J., Bass, A.J., Tabernero, J., et al. (2012). Genomic analysis identifies association of Fusobacterium with colorectal carcinoma. Genome Res. *22*, 292–298.

Kostic, A.D., Chun, E., Robertson, L., Glickman, J.N., Gallini, C.A., Michaud, M., Clancy, T.E., Chung, D.C., Lochhead, P., Hold, G.L., et al. (2013). Fusobacterium nucleatum potentiates intestinal tumorigenesis and modulates the tumor immune microenvironment. Cell Host Microbe *14*, this issue, 207–215.

Le, T.L., Joseph, S.R., Yap, A.S., and Stow, J.L. (2002). Protein kinase C regulates endocytosis and recycling of E-cadherin. Am. J. Physiol. Cell Physiol. *283*, C489–C499.

Lebreton, A., Lakisic, G., Job, V., Fritsch, L., Tham, T.N., Camejo, A., Matteï, P.J., Regnault, B., Nahori, M.A., Cabanes, D., et al. (2011). A bacterial protein

targets the BAHD1 chromatin complex to stimulate type III interferon response. Science *331*, 1319–1321.

Lee, S.H., Hu, L.L., Gonzalez-Navajas, J., Seo, G.S., Shen, C., Brick, J., Herdman, S., Varki, N., Corr, M., Lee, J., and Raz, E. (2010). ERK activation drives intestinal tumorigenesis in Apc(min/+) mice. Nat. Med. *16*, 665–670.

Livak, K.J., and Schmittgen, T.D. (2001). Analysis of relative gene expression data using real-time quantitative PCR and the 2(-Delta Delta C(T)) Method. Methods *25*, 402–408.

Martin, H.M., Campbell, B.J., Hart, C.A., Mpofu, C., Nayar, M., Singh, R., Englyst, H., Williams, H.F., and Rhodes, J.M. (2004). Enhanced Escherichia coli adherence and invasion in Crohn's disease and colon cancer. Gastroenterology *127*, 80–93.

McCoy, A.N., Araújo-Pérez, F., Azcárate-Peril, A., Yeh, J.J., Sandler, R.S., and Keku, T.O. (2013). *Fusobacterium* is associated with colorectal adenomas. PLoS ONE *8*, e53653.

Mohri, Y. (1997). Prognostic significance of E-cadherin expression in human colorectal cancer tissue. Surg. Today *27*, 606–612.

Morin, P.J., Sparks, A.B., Korinek, V., Barker, N., Clevers, H., Vogelstein, B., and Kinzler, K.W. (1997). Activation of beta-catenin-Tcf signaling in colon cancer by mutations in beta-catenin or APC. Science *275*, 1787–1790.

Nithianantham, S., Xu, M., Yamada, M., Ikegami, A., Shoham, M., and Han, Y.W. (2009). Crystal structure of FadA adhesin from Fusobacterium nucleatum reveals a novel oligomerization motif, the leucine chain. J. Biol. Chem. *284*, 3865–3872.

Peifer, M., and Polakis, P. (2000). Wnt signaling in oncogenesis and embryogenesis—a look outside the nucleus. Science *287*, 1606–1609.

Plottel, C.S., and Blaser, M.J. (2011). Microbiome and malignancy. Cell Host Microbe *10*, 324–335.

Sekirov, I., Russell, S.L., Antunes, L.C., and Finlay, B.B. (2010). Gut microbiota in health and disease. Physiol. Rev. *90*, 859–904.

Strauss, J., Kaplan, G.G., Beck, P.L., Rioux, K., Panaccione, R., Devinney, R., Lynch, T., and Allen-Vercoe, E. (2011). Invasive potential of gut mucosa-derived Fusobacterium nucleatum positively correlates with IBD status of the host. Inflamm. Bowel Dis. *17*, 1971–1978.

Swidsinski, A., Khilkin, M., Kerjaschki, D., Schreiber, S., Ortner, M., Weber, J., and Lochs, H. (1998). Association between intraepithelial Escherichia coli and colorectal cancer. Gastroenterology *115*, 281–286.

Tang, W., David, F.B., Wilson, M.M., Barwick, B.G., Leyland-Jones, B.R., and Bouzyk, M.M. (2009). DNA extraction from formalin-fixed, paraffin-embedded tissue. Cold Spring Harb Protoc *2009*, t5138.

Témoin, S., Wu, K.L., Wu, V., Shoham, M., and Han, Y.W. (2012). Signal peptide of FadA adhesin from Fusobacterium nucleatum plays a novel structural role by modulating the filament's length and width. FEBS Lett. *586*, 1–6.

Tremaroli, V., and Bäckhed, F. (2012). Functional interactions between the gut microbiota and host metabolism. Nature *489*, 242–249.

von Kleist, L., Stahlschmidt, W., Bulut, H., Gromova, K., Puchkov, D., Robertson, M.J., MacGregor, K.A., Tomilin, N., Pechstein, A., Chau, N., et al. (2011). Role of the clathrin terminal domain in regulating coated pit dynamics revealed by small molecule inhibition. Cell *146*, 471–484.

Wang, X.W., Buhimschi, C.S., Temoin, S., Bhandari, V., Han, Y.W., and Buhimschi, I.A. (2013). Comparative microbial analysis of paired amniotic fluid and cord blood from pregnancies complicated by preterm birth and early-onset neonatal sepsis. PLoS ONE *8*, e56131.

Wu, S., Lim, K.C., Huang, J., Saidi, R.F., and Sears, C.L. (1998). Bacteroides fragilis enterotoxin cleaves the zonula adherens protein, E-cadherin. Proc. Natl. Acad. Sci. USA *95*, 14979–14984.

Wu, S., Morin, P.J., Maouyo, D., and Sears, C.L. (2003). Bacteroides fragilis enterotoxin induces c-Myc expression and cellular proliferation. Gastroenterology *124*, 392–400.

Wu, S., Rhee, K.J., Albesiano, E., Rabizadeh, S., Wu, X., Yen, H.R., Huso, D.L., Brancati, F.L., Wick, E., McAllister, F., et al. (2009). A human colonic commensal promotes colon tumorigenesis via activation of T helper type 17 T cell responses. Nat. Med. *15*, 1016–1022.

Xu, M., Yamada, M., Li, M., Liu, H., Chen, S.G., and Han, Y.W. (2007). FadA from Fusobacterium nucleatum utilizes both secreted and nonsecreted forms for functional oligomerization for attachment and invasion of host cells. J. Biol. Chem. *282*, 25000–25009.

Yang, J., Zhang, W., Evans, P.M., Chen, X., He, X., and Liu, C. (2006). Adenomatous polyposis coli (APC) differentially regulates beta-catenin phosphorylation and ubiquitination in colon cancer cells. J. Biol. Chem. *281*, 17751–17757.

Zhang, P., Guo, A., Possemato, A., Wang, C., Beard, L., Carlin, C., Markowitz, S.D., Polakiewicz, R.D., and Wang, Z. (2013). Identification and functional characterization of p130Cas as a substrate of protein tyrosine phosphatase nonreceptor 14. Oncogene *32*, 2087–2095. Published online June 18, 2012. http://dx.doi.org/10.1038/onc.2012.220.